JOURNAL OF PHYSICAL ORGANIC CHEMISTRY
J. Phys. Org. Chem. 2005; **18:** 101–109
Published online 21 September 2004 in Wiley InterScience (www.interscience.wiley.com). DOI: 10.1002/poc.858

The search for efficient intramolecular proton transfer from carbon: the kinetically silent intramolecular general base-catalysed elimination reaction of *O*-phenyl 8-dimethylamino-1-naphthaldoximes†

Nabil Asaad, John E. Davies, David R. W. Hodgson,‡ Anthony J. Kirby,* Liisa van Vliet and Laura Ottavi

University Chemical Laboratory, Cambridge CB2 1EW, UK

Received 28 November 2003; revised 19 February 2004; accepted 6 March 2004

ABSTRACT: The ready elimination of phenol/phenoxide from the *O*-phenyl oxime **10E** derived from 8-dimethylamino-1-naphthaldehyde, necessarily involving proton transfer from carbon, is catalysed by the neighbouring NMe_2 group at pH > 9. However, reaction is faster, rather than slower, at lower pH. It is shown that the step involving proton transfer is not cleanly rate determining at any pH: the preferred route involves *syn*/*anti* isomerization to form the more reactive *Z*-isomer. The rate constant for the *anti* elimination cannot be extracted from the available data, so no reliable estimate of effective molarity (EM) is possible. Copyright © 2004 John Wiley & Sons, Ltd.

KEYWORDS: proton transfer; intramolecular general base catalysis; elimination; oxime

INTRODUCTION

Intramolecular reactions are typically faster (and catalytic processes more efficient) than their intermolecular counterparts,[1] so they are of interest as simple models for the reactions which take place when the same functional groups are brought together in enzyme active sites. Intramolecular nucleophilic additions—cyclizations—can be very efficient indeed, with effective molarities (EM) of the order of 10^9 M in unstrained systems, and as high as 10^{13} M in systems in which ground strain is relieved in the transition state for cyclization.[1]

Intramolecular proton transfers are different, typically showing EMs < 10 M, with the important exception of systems in which the product, and hence the transition state leading to it, is stabilized by a strong intramolecular hydrogen bond.[2] These systems are therefore of special interest.[2–4]

Proton transfer is the commonest reaction taking place in enzymes, which generally catalyse reactions in aqueous solution at more or less constant pH. Simple transfers between electronegative centres are mostly diffusion controlled, and unlikely to need catalysis in active sites in rapid exchange with the local medium. However, proton transfers can be slow, and therefore in need of catalysis in biological systems, when concerted with the making or breaking of bonds between heavy atom centres. Examples are the general acid-catalysed hydrolysis of acetals, e.g. **1**,[3] a simple model for the reaction catalysed by the glycohydrolases such as lysozyme, and general base-catalysed elimination reactions **2** (Scheme 1). A special case of the latter process is enolization, **3**, and enzymes such as mandelate racemase, which catalyse the most difficult (intrinsically slow) enolizations have been the focus of much recent attention.[5]

We have shown that the ketonization of the enol ether **4** is catalysed very efficiently by the neighbouring dimethylammonium group (EM > 60 000).[4] So efficient is the proton transfer to and from carbon that the rate-determining step is not the proton transfer but the opening of the intramolecular hydrogen bond of the oxocarbocation intermediate **5** (the geometry of this hydrogen bond is patterned on that of proton sponge[6]).

The logical next step was to examine the enolization of the acids **6** (R = H) and their anions, but we could find no incorporation of deuterium *even into the ester* **6** (α-CH_2, R = Et) under forcing conditions.[7] The geometry is the same as in the efficient system **4**, so we concluded that

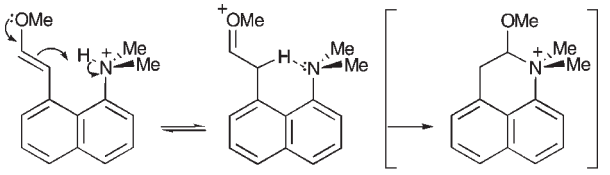

4 5

*Correspondence to: A. J. Kirby, University Chemical Laboratory, Cambridge CB2 1EW, UK.
E-mail: ajk1@cam.ac.uk
†Selected article presented at the Seventh Latin American Conference on Physical Organic Chemistry (CLAFQO-7), 21–26 September 2003, Florianópolis, Brazil.
‡Present address: Department of Chemistry, University of Durham, South Road, Durham DH1 3LE, UK.
Contract/grant sponsor: Engineering and Physical Sciences Research Council of Great Britain.

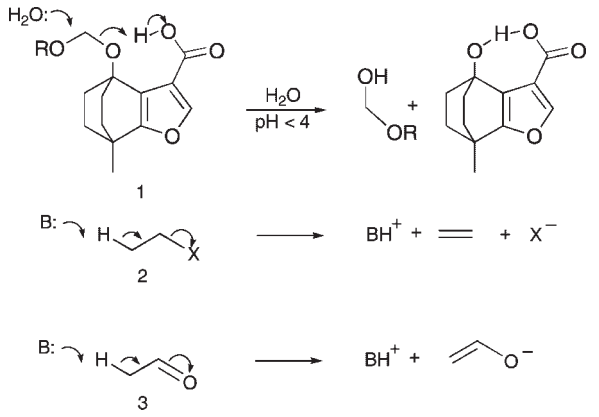

Scheme 1

exchange is not observed because proton return from the enolate intermediate **7**, to regenerate the starting material, is much faster than the opening of the intramolecular hydrogen bond needed for exchange of the NH^+ with solvent.[7]

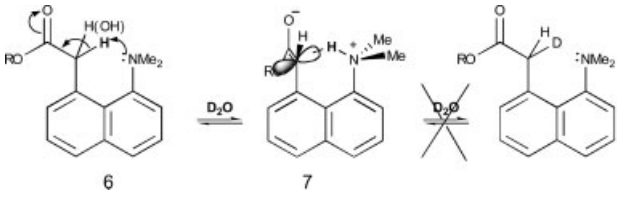

In a further attempt to observe efficient intramolecular proton transfer using this basic system, we prepared the vinyl bromide **8** (D = H, and the labelled form shown),[8] designed to support the efficient elimination of HBr. However, reaction gave not the alkyne but the heterocycle **9**. The mechanism probably involves an initial nucleophilic addition of the dimethylamino group to form a five-membered ring: in any event, the target hydron is still present in the product, so the desired proton transfer has not occurred.[8]

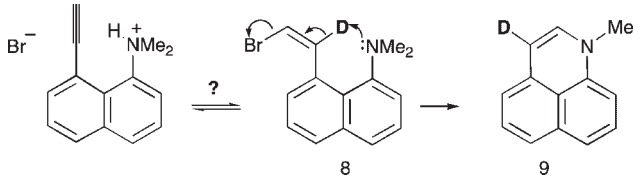

We report our first successful attempt to follow an elimination reaction in a system based on proton sponge. 8-Dimethylamino-1-naphthaldehyde is the common intermediate in the synthesis of a number of the compounds described above, so it was a relatively simple matter to prepare oxime derivatives (general formula **10***, geometry may be *Z* or *E*). Of three compounds prepared (obtained as the *E*-isomers, no doubt for steric reasons), the acetate was inconveniently reactive and the methoxy derivative was hydrolysed faster than it eliminated methanol. However, the *O*-phenyl derivative **10E** was converted quantitatively to the nitrile **11** within hours in aqueous solution at 30 °C (Scheme 2).

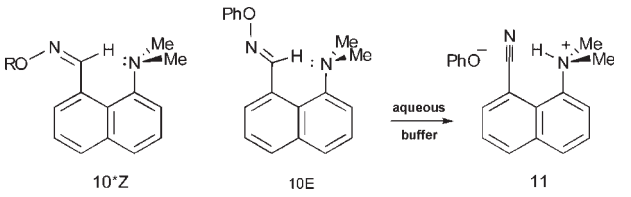

Scheme 2

RESULTS AND DISCUSSION

The elimination of phenol (or phenoxide) from **10E** to form the nitrile **11** (Scheme 2) was conveniently studied [in 50% (v/v) acetonitrile–water, for solubility reasons] at 60 °C and ionic strength 0.1 M (KCl). Since system **10** was designed to support an efficient intramolecular general base-catalysed proton transfer from carbon, it was expected to react in the free base form, thus at pHs above the pK_a of the dimethylammonium group. In practice, the pH–rate profile for the elimination (Fig. 1) shows a reaction that is *slower* at high pH. Reaction is slow also at low pH, as expected if rapid elimination depends on the presence of the dimethylamino group in its free base form. However, the dimethylamino group is also (presumably) protonated in the pH-independent region between pH 2 and 8: only the higher of the two apparent pK_as (1.26 and 8.61) derived from the pH–rate profile can reasonably be assigned to the dimethylammonium group (see below). Hence, the mechanism appears not to be a simple elimination process.

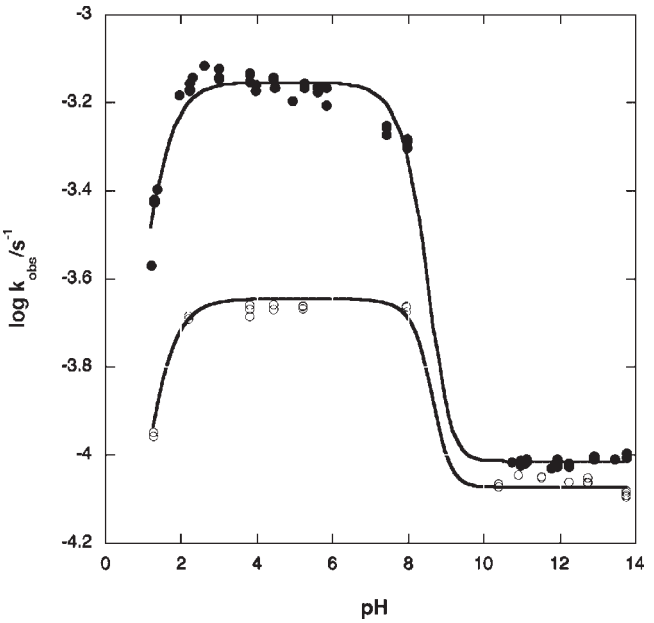

Figure 1. pH–rate profiles for the elimination reactions of **10E**, (filled circles) and *d*-**10E** (open circles), to form **11**: in 50% (v/v) acetonitrile–H_2O at 60°C and ionic strength 0.1M (KCl). The curves represent calculated fits based on the mechanism discussed below

Reaction mechanism

Proton transfers to and from carbon typically show substantial and informative primary deuterium isotope effects, so we also measured the pH–rate profile for elimination from the deuterio-compound ***d*-10E** (see Fig. 1 and Table 1). The observed kinetic deuterium isotope effects tell us that proton transfer is not rate determining for the elimination reaction of **10E**, and probably not exclusively rate determining for the faster reaction of the conjugate acid, $\mathbf{10EH}^+$.

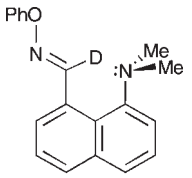

d-10E

In the high pH region (pH > 9), there is no significant primary deuterium isotope effect ($k_H/k_D = 1.13 \pm 0.04$). For comparison, the most closely analogous reactions, the eliminations of pivalate[9] and benzyloxide[10] from the corresponding (*E*)-*O*-acyl (alkyl) oximes of benzaldehyde catalysed by DBU, show $k_H/k_D = 2.7$ and 3.3, respectively. For the corresponding *Z*-isomers, which react 20 000 (36 000) times faster, $k_H/k_D = 7.8$ and 7.3, respectively.[9,10]

In the plateau region between pH 2 and 8, we observe a substantial deuterium isotope effect ($k_H/k_D = 3.08 \pm 0.11$). This *is* consistent with rate-determining elimination from **10E**; however, this is unlikely to be the correct explanation, because reaction is faster, rather than slower, than that of the free base form above pH 9. The elimination step catalysed by the dimethylamino group of the free base **10E** is expected to be faster than that of its conjugate acid, but overall elimination is slower at pH > 9, because the proton transfer step is not rate determining in this pH region.

The plateau reaction

The *O*-phenyl oxime **10E** has three possible conjugate acids. Apart from the predominant dimethylammonium

Table 1. Rate data for the conversion of oxime **10E** to the nitrile **11**, in 50% (v/v) acetonitrile–water at 60 °C and ionic strength 1.0 M (data in s^{-1})

	Reaction of **10E**			Reaction of ***d*-10E**	
pH	Log k_{obs}	pH	Log k_{obs}	pD	Log k_{obs}
1.2100	−3.5705	5.8200	−3.1651	1.2800	−3.9593
1.2800	−3.4189	5.8200	−3.2075	1.2800	−3.9494
1.2800	−3.4265	7.4200	−3.2576	2.2000	−3.6926
1.3600	−3.3978	7.4200	−3.2740	2.2000	−3.6854
1.9500	−3.1833	7.4200	−3.2548	4.4500	−3.6598
2.2000	−3.1703	7.9600	−3.3021	4.4500	−3.6708
2.2000	−3.1737	7.9600	−3.2892	3.8200	−3.6861
2.2000	−3.1571	7.9600	−3.2828	3.8200	−3.6702
2.3100	−3.1438	10.730	−4.0150	3.8200	−3.6609
2.6000	−3.1168	10.980	−4.0230	10.920	−4.0462
2.9800	−3.1416	10.980	−4.0118	7.9600	−3.6636
2.9800	−3.1455	10.980	−4.0148	7.9600	−3.6766
2.9800	−3.1233	11.090	−4.0189	7.9600	−3.6655
3.8200	−3.1523	11.110	−4.0112	12.260	−4.0622
3.8200	−3.1352	11.110	−4.0179	13.770	−4.0814
3.8200	−3.1337	11.780	−4.0310	13.770	−4.0866
3.9700	−3.1734	11.950	−4.0198	13.770	−4.0927
3.9700	−3.1591	11.950	−4.0113	13.770	−4.0952
4.4500	−3.1451	11.950	−4.0249	10.400	−4.0735
4.4500	−3.1466	12.260	−4.0243	10.400	−4.0665
4.4500	−3.1417	12.260	−4.0272	10.400	−4.0736
4.4600	−3.1650	12.260	−4.0197	13.770	−4.0814
4.9600	−3.1950	12.920	−4.0046	13.770	−4.0866
5.2500	−3.1653	12.920	−4.0105	13.770	−4.0927
5.2500	−3.1576	12.920	−4.0020	13.770	−4.0952
5.2500	−3.1559	13.460	−4.0101	12.750	−4.0647
5.6100	−3.1639	13.760	−3.9966	12.750	−4.0625
5.6100	−3.1751	13.760	−4.0064	12.750	−4.0519
5.6100	−3.1659			11.530	−4.0526
				11.530	−4.0503
				5.2300	−3.6638
				5.2300	−3.6626
				5.2300	−3.6687

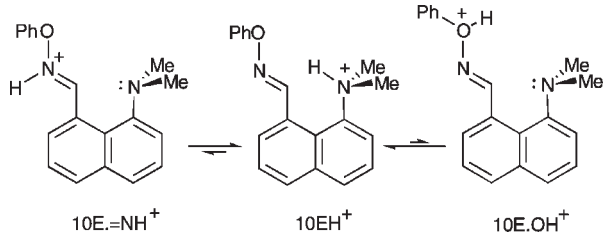

Scheme 3

form **10EH**$^+$, the oxime group can be protonated, on either nitrogen or oxygen (Scheme 3). The *N*-protonated form **10E**·**═NH**$^+$ might be expected to be a relatively strong acid (the pK_a of the oxime derived from 9-formylfluorene is -1.62[11]) and the *O*-protonated form **10E** · **OH**$^+$ a very strong acid, with p$K_a < -7$.[12] If the pK_a of the major species **10EH**$^+$ is 8.61, the equilibrium constant for the formation of **10E** · **OH**$^+$ will be $<10^{-15}$, requiring a first-order rate constant for the elimination of phenol of the order of $10^{12}\,s^{-1}$ from a species existing for only a few vibrations. If not formally impossible, such a rate constant is highly unlikely (particularly for a *syn*-elimination, which might be expected to be significantly slower than the corresponding *trans*-elimination reaction).

A much more likely initial reaction for the conjugate acid **10EH**$^+$, consistent with the known behaviour of *peri*-disubstituted systems,[13] and explaining why it reacts faster than the basic form, is cyclisation of the *N*-protonated oxime **10E**·**═NH**$^+$. This will generate **12** (Scheme 4), making possible free rotation about what was the C═N bond of the oxime. Compound **12** can open either to regenerate **10E**·**═NH**$^+$ or to give the *Z*-isomer **10Z** of the oxime (via **10Z**·**═NH**$^+$). This opens the way to a new, low-energy pathway because *trans*-elimination from the *Z*-isomers of oximes derived from aromatic aldehydes is known to be much faster than *syn*-elimination from the *E*-isomers, as discussed above. Hence we consider that the reaction between pH 2 and 8 goes through **12** (Scheme 4). The reaction of the neutral species **10E** is presumed to go by a similar mechanism via the zwitterionic intermediate **12** ±. The reaction of the conjugate acid **10EH**$^+$ is faster because the cyclisation of **10E**·**═NH**$^+$ is faster than that of **10E**.

Scheme 4 provides a qualitative framework for the more quantitative discussion of the mechanism. {Note: A referee suggests that the path to the nitrile (Scheme 4) could involve a Lossen-type rearrangement of **12** ±, with hydride migration concerted with the departure of phenoxide (generating initially the [HN═C—N$^+$Me$_2$] intermediate). We considered[8] the corresponding mechanism for the rearrangement of **8**, which involved the departure of Br$^-$, a much better leaving group, and required the NMe$_2$ group rather than hydride to migrate. Similar considerations apply to the rearrangement of **12** ±, but the alternative mechanism cannot formally be ruled out.}

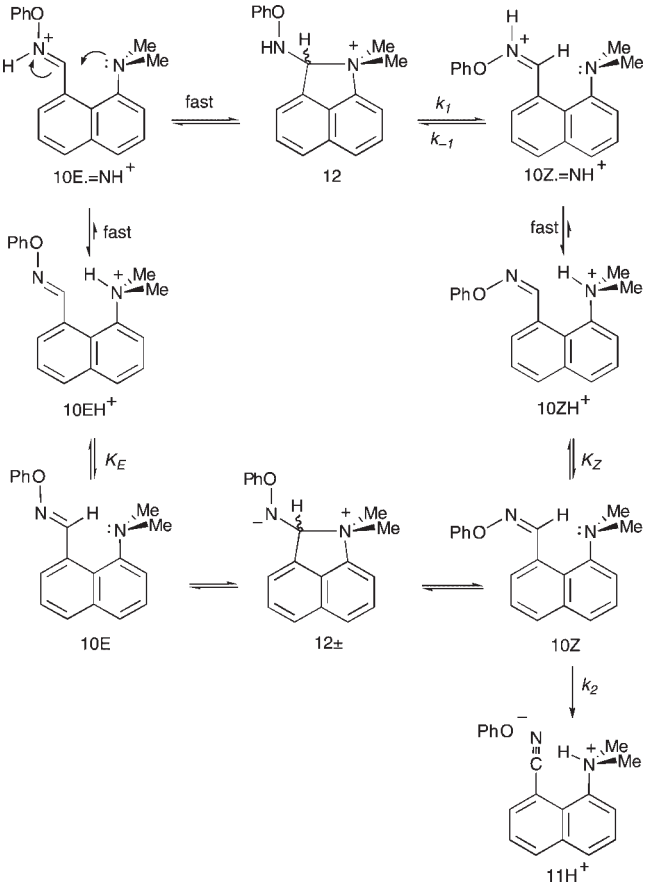

Scheme 4

Two parameters are of particular interest, the apparent pK_as of 1.26 and 8.61, and the primary kinetic isotope effects in the two pH-independent regions.

pK_as

We have not been able to measure pK_as convincingly for **10EH**$^+$: it is rapidly degraded when titrated with base, and the changes in the UV spectrum with pH are not simple. (There is no ^{1}H NMR evidence for the formation of significant amounts of a third species under the reaction conditions, either for **10E** of for the more stable *O*-methyl oxime.) The apparent pK_as (1.26 and 8.61) are very different from those expected for the individual dimethylamino and oxime groups of **10E**, so they must represent either kinetic pK_as or values shifted by intramolecular interactions between the groups. Such intermolecular interactions are well known in 1,8-disubstituted naphthalenes,[14] and anomalous pK_as generally result from the formation of strong hydrogen bonds between electronegative *peri*-substituents. In the case of **10EH**$^+$ the strongest intramolecular hydrogen bond possible is between the Me$_2$NH$^+$ group and the oxime N, and this is observed (not unexpectedly) in the crystal structure

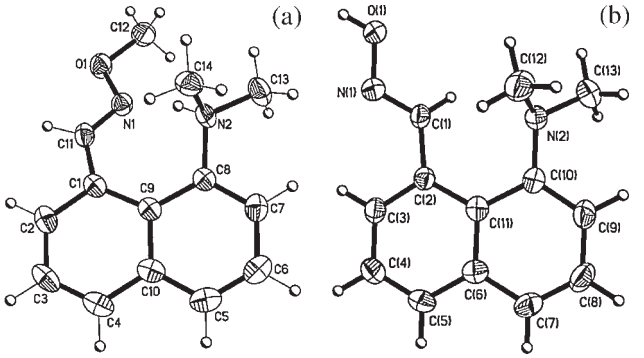

Figure 2. (a) Molecular structure of **13EH**$^+$ (crystallized as the tetrafluoroborate salt) and (b) the parent oxime **14** (free base form). ORTEP: ellipsoids are drawn at the 30% probability level and hydrogen atoms are represented as spheres of radius 0.12 Å. For details, see the Experimental section

of the tetrafluoroborate salt of the *O*-methyl oxime **13EH**$^+$ [Fig. 2(a)].

The N–H···N angle is 164.8° and the N···N distance is 2.628 Å (at 150 K), close to those [160(3)° and 2.571 Å at 120 K] of the very strong hydrogen bond of the conjugate acid of proton sponge [1,8-bis(dimethylamino)naphthalene].[15] However, this is achieved in **13EH**$^+$ only at the expense of significant distortion of the naphthalene framework: the torsion angle C(1)—C(9)—C(8)—N(2) is over 20° (the conjugate acid of proton sponge is almost planar) and the bond angles C(9)—C(1)—N(1) and C(9)—C(8)—N(2) are expanded to 128.9° and 124.5°, respectively, to accommodate the proton. {The N···N distance of closest approach in the relevant conformer of the oxime [Fig. 2(b)] would be an implausible 1.89 Å.} As a result, the thermodynamic stability of the H-bond, and hence the effect on the pK_a of **10EH**$^+$, is expected to be reduced.

The *O*-methyl oxime **13E** is considerably more stable than the *O*-phenyl derivative **10E**, and so offers increased scope for physical measurements. Unfortunately, it behaves differently under the conditions: it is not sufficiently soluble in 50% aqueous acetonitrile, so measurements were made in 10% dioxane. However, in this solvent it did not undergo the elimination of interest: hydrolysis of the oxime group to the parent aldehyde is faster. Titration at low pH reveals a pK_a of 3.22 ± 0.07 (in 10% dioxane at room temperature), falling to 2.34 ± 0.16 in 50% acetonitrile (adding 0.5 equiv. of HCl to a solution of **13EH**$^+$ gave a solution of pH ca 2.6). This is consistent with a pK_a of 1.26 at 60 °C for the *O*-phenyl derivative. This evidence suggests that the lower of the two apparent pK_as of **10EH**$^+$ is a true pK_a; we have no conclusive evidence that this is the case for the higher pK_a at 8.61.

Mechanism of the elimination reaction of 10

A suggested mechanism is outlined in Scheme 4. At high pH, above the pK_a of the dimethylammonium group, reaction involves rate-determining *anti-syn* isomerization of **10E** to **10Z**, via **12** $\pm$, followed by the rapid elimination of phenoxide from the less abundant but far more reactive neutral isomer **10Z**. No significant primary isotope effect is observed because the C—H bond is not broken in the rate-determining step. At lower pHs (on the plateau between pH 2 and 8) cyclization, leading to the (reversible) isomerization of **10EH**$^+$, is faster, and rapid elimination from **10Z** (k_2) competes with its recyclization, via **10ZH**$^+$. (Apart from undergoing elimination much more rapidly **10Z** is also expected to be substantially less basic than **10E** because it is unable, for geometric reasons, to form the intramolecular hydrogen bond that we consider responsible for the unusually high pK_a of **10EH**$^+$. We have no direct evidence on this point.) We suggest that the observed primary kinetic isotope effect (3.08 ± 0.11) reflects a larger figure (of around 7) for the *anti* elimination of **10Z**, reduced by the negligible isotope effect expected for its (partially rate-determining) recyclization to **12**, which must go at a comparable rate (via **10ZH**$^+$).

We see no evidence, from ^{1}H NMR measurements in D_2O (at room temperature) under the reaction conditions, that **12** is formed in significant concentrations in the plateau region. The parent aldehyde **14** is largely (2:1 mixture observed by ^{1}H NMR) converted to the cyclic aminal **15** in $CDCl_3$ in the presence of 10% CF_3COOD (Scheme 5);[13] as shown by the reduced intensity of the oxime N=C*H* singlet, the appearance of a new (methine) proton signal at δ 7.0, and the doubling and downfield shift of the *N*-methyl proton signal.

None of these NMR indicators is observed for **10E** or for the *O*-methyl oxime in the plateau region. The oxime singlet at δ 9.46 does disappear, essentially completely, in 0.1 M DCl, to be replaced by a broad signal at δ 8.13 (and weaker signals at δ 5.1–5.3, initially obscured by the HDO peak). This intriguing result is most likely only indirectly relevant to the mechanism at higher pH, although we know that the species present is relatively unreactive.

The calculated curves shown in Fig. 1 represent the fits derived on the basis of Scheme 4. The data in the plateau region (pH 1–9) were fitted to the simplified Eqn (1) based on Scheme 6, using the steady-state assumption.

We assume that all proton transfers between O and N centres are fast, and that k_1, the opening of the intermediate **12** (Scheme 4) to give the thermodynamically less stable isomer of the oxime, is the rate-determining

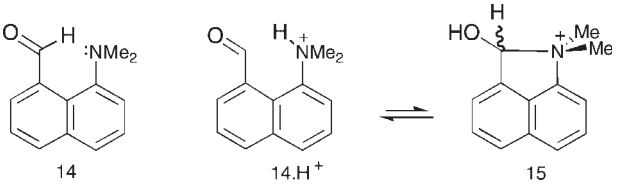

Scheme 5

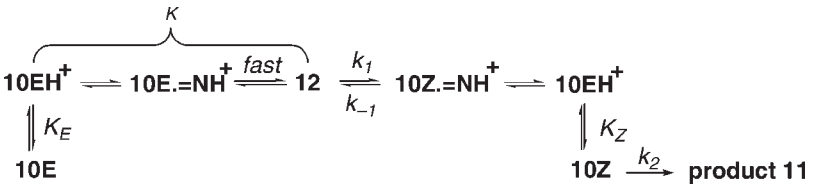

Scheme 6

step for the isomerization process. Then **10E** is in rapid pre-equilibrium with **12** (K_{12} is the equilibrium constant for the formation of **12** from **10EH**$^+$), and we can write (for the plateau reaction):

$$k_{obs} = k_1 K_{12}[\mathbf{10EH}^+] \times k_2[\mathbf{10Z}]/(k_{-1}[\mathbf{10Z} \cdot = \mathbf{NH}^+] + k_2[\mathbf{10Z}]) \quad (1)$$

The pH-independent reaction above pH 9 is allowed for by the addition of a separate term.

The same procedure gives a good fit for the reaction of ***d*-10E**. The rate and equilibrium constants derived from the fits of the data for **10E** and its deuterated form ***d*-10E** are given in Table 2. The derived rate constants k_1, k_{-1} and k_2 give errors larger than the figures quoted and do not represent unique solutions, although relative values should be meaningful. The derived 'pK_as' match closely the apparent pK_as, except that the values for **10E** and **10Z** are reversed. The resultant deuterium isotope effects fall within $\pm 20\%$ of unity for k_1, for k_{-1} and for the rate constant k_0 at high pH, but for k_2, the elimination reaction of the reactive isomer **10Z** $k_H/k_D = 7.9$. This is the value expected for this process according to the closest precedent available (see above).[10]

CONCLUSIONS

The mechanism of the elimination of phenol from oxime **10E** is not characterized down to the last detail, but we have established (i) that reaction is subject to the expected catalysis by the neighbouring dimethylamino group, (ii) that *syn* elimination from the *E*-isomer is not observed (and is therefore slower than the reactions that are observed), (iii) that the proton transfer step is not cleanly rate determining at any pH and (iv) that the preferred route involves isomerisation to the more reactive *Z*-isomer. The rate constant for the *anti* elimination cannot be extracted from the available data, so no reliable estimate of effective molarity is possible.

Table 2. Derived rate and equilibrium constants for the elimination reactions of **10E** and its deuterated form in 50% (v/v) acetonitrile–water at 60 °C

Parameter	**10E**	***d*-10E**	k_H/k_D
k_1K_{12}	6540	6900	0.95
k_2	4440	562	7.9
k_{-1}	0.0546	0.0556	0.79
pK_a (EH^+)	1.26 ± 0.04	1.25 ± 0.04	0.98
pK_a (ZH^+)	8.61	8.25	0.44
k_0 (pH > 9)	$(9.66 \pm 0.15) \times 10^{-5}$	$(8.43 \pm 0.10) \times 10^{-5}$	1.14
R	0.997	0.996	

EXPERIMENTAL

Syntheses

All solvents were dried by standard procedures and distilled and all glassware was oven-dried before use. Potentially moisture-sensitive reactions were carried out under an atmosphere of argon. Analytical thin-layer chromatography was performed on precoated 0.25 mm Merck Kieselgel 60F_{254} plates. Flash column chromatography was carried out using Merck Kieselgel 60 (230–400 mesh). Melting-points were measured on a Stuart Scientific SMP1 melting-point apparatus and are uncorrected.

NMR spectra were recorded on Bruker DPX400, DRX400 and DRX500 FT spectrometers at probe temperatures of 27 °C unless stated otherwise. The solvent signal was used as internal deuterium lock. Chemical shifts are quoted downfield from δ (tetramethylsilane) = 0 ppm for ^{1}H and ^{13}C NMR. The multiplicity of first-order signals is indicated by standard notation. Broadband proton decoupling was used for ^{13}C NMR. Infrared spectra were recorded on Perkin-Elmer 1600 FT-IR and Spectrum One FT-IR spectrometers. Mass spectra were recorded on Kratos MS890 (EI), Kratos FAB MS890 (FAB), MSI Concept IH (EI and LSIMS), Bruker Bio-apex II FT-ICR (ESI, LSIMS and EI) and ESI Micromass Q-TOF (+ES) mass spectrometers.

[1′-D]-8-N,N-Dimethylamino-1-naphthaldehyde. N,N- Dimethylamino-1-naphthylamine (**14**, 3.0 g, 17.5 mmol) was dissolved in diethyl ether (180 cm^3) and cooled to −78 °C. *n*-Butyllithium (15 cm^3, 2.3 M solution in hexane, 2 equiv.) was added dropwise and the mixture stirred for 30 h, warming to room temperature. A white precipitate formed from the yellow solution. The mixture was again cooled to −78 °C and a solution of [1-D]-dimethylformamide (1.5 cm^3, 1.1 equiv.), was cannulated in at −78 °C. Stirring was continued for a further 3 h. Methanol (20 cm^3) was added and the mixture allowed to warm

to room temperature. Distilled water (80 cm^3) was added and the solution basified (KOH). The layers were shaken and separated, then the aqueous layer extracted with hexane ($2 \times 50\ cm^3$). The combined organic layers were washed (brine), dried ($MgSO_4$) and evaporated to near dryness. A small volume of toluene was added and the crude product was stored in a freezer to yield the aldehyde as transparent pale-yellow plates (1.21 g). The mother liquor was chromatographed (SiO_2, Et_2O–hexane, 1:3) to yield further aldehyde as a yellow powder (0.98 g, 62% overall), m.p. 80–82 °C; R_F (Et_2O–hexane, 1:3) 0.13; NMR, δ_H ($CDCl_3$) 8.22 (1 H, d, *J* 7, ArH), 7.89 (1 H, dd, *J* 8 and 1, ArH), 7.63 (1 H, dd, *J* 8 and 1, ArH), 7.54 (1 H, dd, *J* 7 and 1, ArH), 7.51–7.45 (1H, m, ArH), 7.31 (1 H, dd, *J* 7 and 1, ArH) and 2.68 (6H, s, NMe_2); δ_C ($CDCl_3$) 191.4 (t, *J* 29, C═O), 150.3, 137.2, 135.0, 130.9 (CH), 129.3, 126.7 (CH), 125.9 (CH), 125.0 (CH), 124.7 (CH), 118.2 (CH), 44.9 (NMe_2); IR (Nujol), ν_{max} 1649 (C═O); MS, *m/z* (+ES) 201.11310 ($C_{13}H_{12}DNO \cdot H^+$ requires 201.11302).

*O-Phenyl-8-N,N-dimethylamino-1-naphthaldoxime (***10E***).* *N*,*N*-Dimethylamino-1-naphthaldehyde (48.8 mg, 0.24 mmol), *O*-phenylhydroxylamine hydrochloride (64 mg, 2 equiv.) and sodium acetate (75 mg, 4 equiv.) were dissolved in methanol (15 cm^3) and the mixture was stirred at room temperature for 15 min. The reaction mixture was extracted with hexane ($3 \times 30\ cm^3$) and the combined hexane layers were washed with brine (30 cm^3), dried ($MgSO_4$) and evaporated under vacuum, maintaining the temperature below 40 °C. The crude product was chromatographed (SiO_2, Et_2O-hexane, 1:3) and freeze-drying yielded the oxime ether as pale-yellow needles (54.1 mg, 76%), R_F (Et_2O–hexane, 1:3) 0.35; which decomposed on heating. NMR, δ_H ($CDCl_3$) 9.56 (1 H, s, CH═N), 7.88 (1 H, dd, *J* 8.0 and 1, ArH), 7.73 (1 H, dt, *J* 7 and 1, ArH), 7.58 (1 H, dd, *J* 7 and 1, ArH), 7.46 (1 H, t, *J* 7, ArH), 7.42 (1 H, t, *J* 7, ArH), 7.37–7.28 (4 H, m, ArH), 7.25 (1 H, m, ArH), 7.04 (1 H, tt, *J* 7 and 1, ArH), 2.72 (6H, s, NMe_2); δ_C ($CDCl_3$) 160.3 (C_{Ph}—O), 155.4 (C═N), 151.6 (C_{Ar}—N), 136.1 (C_{Ar}C═N), 130.9 (CH), 129.7 (C_{Ph}—H), 128.9, 128.7, 127.9 (CH), 126.6 (CH), 126.0 (CH), 124.8 (CH), 122.2 (CH), 117.6 (CH), 115.0 (C_{Ph}—H) and 45.6 (CH_3—N); IR (Nujol), ν_{max} 1605, 1583; MS, *m/z* (+EI) 290.1416 ($C_{19}H_{18}N_2O$ requires 290.1419).

*[1′-D]-O-Phenyl-8-N,N-dimethylamino-1-naphthaldoxime (***d-10E***).* This was prepared by the above method using [1′-D]-*N*,*N*-dimethylamino-1-naphthaldehyde (49.1 mg, 24.4 mmol) to yield the oxime ether as pale-yellow needles (61.7 mg, 87%); NMR, δ_H ($CDCl_3$) 7.87 (1 H, dd, *J* 8.0 and 1, ArH), 7.75 (1 H, dt, *J* 7 and 1, ArH), 7.58 (1 H, dd, *J* 7 and 1, ArH), 7.48 (1 H, t, *J* 7, ArH), 7.43 (1 H, t, *J* 7, ArH), 7.38–7.29 (4 H, m, ArH), 7.25 (1 H, m, ArH), 7.04 (1 H, m, ArH), 2.72 (6H, s, NMe_2); δ_C ($CDCl_3$) 160.3 (C_{Ph}—O), 151.6 (C_{Ar}—N), 136.8 (C_{Ar}C═N), 131.0, 129.7 (C_{Ph}—H), 128.9, 128.7, 127.9 (CH), 126.6 (CH), 126.0 (CH), 124.8 (CH), 122.2 (CH), 117.6 (CH), 115.0 (C_{Ph}—H), 45.6 (CH_3—N).

*O-Methyl-8-N,N-dimethylamino-1-naphthaldoxime (***13E***).* *N*,*N*-Dimethylamino-1-naphthaldehyde (292 mg, 1.46 mmol), *O*-methylhydroxylamine hydrochloride (240 mg, 2 equiv.) and sodium acetate (480 mg, 4 equiv.) were dissolved in methanol (20 cm^3) and the mixture was stirred at room temperature for 1 h. Brine (5 cm^3) and distilled water (10 cm^3) were added and the mixture was extracted with hexane ($3 \times 30\ cm^3$). The combined organic extracts were washed with brine (30 cm^3), dried ($MgSO_4$) and evaporated under vacuum. The crude product was chromatographed (SiO_2, Et_2O–hexane, 1:3) and freeze-drying yielded the oxime ether as pale-yellow needles (290 mg, 87%), R_F (Et_2O–hexane, 1:3) 0.29, which decomposed on heating. NMR, δ_H ($CDCl_3$) 9.21 (1 H, s, CH═N), 7.81(1 H, dd, *J* 7 and 1, ArH), 7.64 (1 H, dd, *J* 7 and 1, ArH), 7.56 (1 H, dd, *J* 8 and 1, ArH), 7.43 (1 H, t, *J* 8, ArH), 7.40 (1 H, t, *J* 8, ArH), 7.20 (1 H, dd, *J* 8 and 1, ArH), 4.00 (3 H, s, OMe) and 2.68 (6H, s, NMe_2); δ_C ($CDCl_3$) 150.8 (C═N), 150.1 (C_{Ar}—N), 134.6 (C—C═N), 128.9 (CH), 127.8, 127.0, 125.7 (CH), 124.8 (CH), 124.3 (CH), 123.0 (CH), 115.6 (CH), 60.4 (CH_3—O) and 43.8 (CH_3—N); IR (Nujol), ν_{max} 1597, 1577; MS, *m/z* (+EI) 228.1264 ($C_{14}H_{16}N_2O$ requires 228.1263).

*Tetrafluoroborate salt of O-methyl-8-N,N-dimethylamino-1-naphthaldoxime (***13EH$^+$***).* *O*-Methyl-8-*N*,*N*-dimethylamino-1-naphthaldoxime (20 mg) was dissolved in diethyl ether (1 cm^3). Hydrogen tetrafluoroborate [$\sim$0.1 cm^3, 54% (w/w) in diethyl ether] was added dropwise until precipitation ceased. The liquid was decanted off and the white precipitate dissolved in methanol ($\sim$0.2 cm^3). A layer of diethyl ether ($\sim$1 cm^3) was carefully deposited on top of the methanol layer and the solution allowed to crystallize as colourless plates. The compound decomposed on heating.

*8-Cyano-N,N-dimethylamino-1-naphthylamine (***11***).* 8-*N*,*N*-Dimethylamino-1-naphthylaldoxime (60 mg, 0.28 mmol) was dissolved in dichloromethane (2 cm^3). Pyridine (0.1 cm^3, 5 equiv.) and freshly distilled acetic anhydride (0.5 cm^3, 5 equiv.) were added and the mixture was heated at 50 °C for 2 h. The reaction mixture was washed with dilute hydrochloric acid ($3 \times 5\ cm^3$) and saturated sodium hydrogencarbonate solution ($3 \times 5\ cm^3$) and dried ($MgSO_4$). The solvent was removed under vacuum to yield the nitrile as a yellow solid (47 mg, 85%), m.p. 75–76 °C.[16] NMR, δ_H ($CDCl_3$) 8.01 (1 H, d, *J* 8, ArH), 7.96 (1 H, d, *J* 7, ArH), 7.60 (1 H, d, *J* 8, ArH), 7.52–7.45 (2 H, m, ArH), 7.33 (1 H, d, *J* 7, ArH) and 2.82 (6H, s, NMe_2); δ_C ($CDCl_3$) 151.4, 137.0 (CH), 136.1, 134.3 (CH), 130.1, 128.3 (CH), 126.0 (CH), 125.4 (CH), 121.5, 119.8 (CH), 109.1 (C—N) and 46.6 (NMe_2); IR,

ν_{max} (CH_2Cl_2) 1612, 1590, 1574; MS, *m/z* (EI) 196.0999 ($C_{13}H_{12}N_2$ requires 196.1000).

Kinetic measurements

All buffer reagents were of analytical-reagent grade. Deionized water was doubly distilled in all-glass apparatus and degassed with argon. KOH and HCl stock solutions (2 mol dm^{-3}) were made by dilution of BDH Convol concentrates. Buffer solutions were made by appropriate dilution in grade A volumetric flasks: the appropriate quantity of KCl was added to adjust the ionic strength to 0.10 M. Dioxane was freshly distilled from $NaBH_4$ prior to use; the cosolvent content is quoted as percentage (v/v). The reaction was followed at 60 °C in 50% aqueous MeCN using HCl, KOH and formate, acetate, phosphate, Tris and carbonate buffers. The pH of each buffer solution was recorded at the temperature used in the kinetic investigation, using a Radiometer PHM82 pH meter fitted with a Russell CTWL electrode calibrated to standard buffer solutions. Rate data are given in Table 1.

UV–visible spectroscopic data were recorded using a Varian Cary 3 spectrometer fitted with a thermostated cell holder maintained at the temperature stated. Stock solutions ($\sim 5 \times 10^{-3}$ mol dm^{-3}) of kinetic substrates were prepared in acetonitrile. The stock solution (10 µl) was added to preheated buffer solution (2 cm^3) in a quartz cuvette (1.0 cm pathlength) for each kinetic run. Repetitive wavelength scans were carried out for each kinetic substrate in a series of buffer solutions to determine whether the reaction exhibited one or more isosbestic points and to allow the selection of an appropriate wavelength at which to record absorbance–time data. Experimental data were fitted to the first-order rate law equation using Kaleidagraph v. 3.08 (Synergy Software), assuming that the observed change in absorbance was the result of conversion of reactant to product; accuracies quoted are ± 1 standard deviation. No buffer catalysis was observed in this work. Multi-parameter curve fitting for the plateau region data was based on Eqn (1) and used the Kaleidagraph implementation of the Levenberg–Marquardt algorithm.

Crystal structure determinations

Selected bond lengths and angles, relevant to the interacting *peri*-substituent groups, are given in Tables 3 and 4.

Crystal data for **13H**$^+$. $C_{14}H_{17}BF_4N_2O$, $M = 316.11$, triclinic, space group *P*-1 (No. 2), $a = 7.5686(6)$, $b = 8.1133(6)$, $c = 12.2631(6)$ Å, $\alpha = 98.757(5)$, $\beta = 92.343(4)$, $\gamma = 99.341(3)°$, $U = 732.72(9)$ $Å^3$, $Z = 2$, λ(Mo Kα) = 0.124 mm^{-1}, 6082 reflections measured at 180(2) K using an Oxford Cryosystems Cryostream cooling apparatus, 2509 unique ($R_{int} = 0.043$); $R_1 = 0.059$, $wR_2 = 0.151$ [$I > 2\_(I)$]; goodness-of-fit on F^2,

Table 3. Selected bond lengths and angles for **13H**$^+$ [Fig. 2(a)]

Bond lengths (Å)					
O(1)—N(1)	1.401(3)	N(2)—C(13)	1.497(3)	C(1)—C(11)	1.469(3)
O(1)—C(12)	1.433(3)	N(2)—C(14)	1.500(3)	C(7)—C(8)	1.371(4)
N(1)—C(11)	1.274(3)	C(1)—C(2)	1.389(3)	C(8)—C(9)	1.432(3)
N(2)—C(8)	1.475(3)	C(1)—C(9)	1.450(3)	C(9)—C(10)	1.435(3)
Bond angles (°)					
N(1)—O(1)—C(12)	108.3(2)	C(2)—C(1)—C(9)	118.7(2)	C(9)—C(8)—N(2)	119.7(2)
C(11)—N(1)—O(1)	112.5(2)	C(2)—C(1)—C(11)	111.6(2)	C(8)—C(9)—C(10)	115.1(2)
C(8)—N(2)—C(13)	115.7(2)	C(9)—C(1)—C(11)	128.9(2)	C(8)—C(9)—C(1)	128.3(2)
C(8)—N(2)—C(14)	111.2(2)	C(7)—C(8)—C(9)	122.3(2)	C(10)—C(9)—C(1)	116.6(2)
C(13)—N(2)—C(14)	111.0(2)	C(7)—C(8)—N(2)	117.6(2)	N(1)—C(11)—C(1)	124.5(2)

Table 4. Selected bond lengths and angles for **14** [Fig. 2(b)]

Bond lengths (Å)					
O(1)—N(1)	1.422(3)	N(2)—C(12)	1.464(4)	C(6)—C(11)	1.428(4)
N(1)—C(1)	1.275(4)	C(1)—C(2)	1.477(4)	C(9)—C(10)	1.373(5)
N(2)—C(10)	1.419(4)	C(2)—C(3)	1.374(4)	C(10)—C(11)	1.443(5)
N(2)—C(13)	1.450(4)	C(2)—C(11)	1.439(4)		
Bond angles (°)					
C(1)—N(1)—O(1)	110.8(2)	C(3)—C(2)—C(11)	119.1(3)	N(2)—C(10)—C(11)	118.5(3)
C(10)—N(2)—C(13)	115.7(3)	C(3)—C(2)—C(1)	116.2(3)	C(6)—C(11)—C(2)	117.5(3)
C(10)—N(2)—C(12)	113.1(3)	C(11)—C(2)—C(1)	124.5(3)	C(6)—C(11)—C(10)	117.6(3)
C(13)—N(2)—C(12)	111.9(3)	C(9)—C(10)—N(2)	121.8(3)	C(2)—C(11)—C(10)	124.9(3)
N(1)—C(1)—C(2)	117.4(3)	C(9)—C(10)—C(11)	119.7(3)		

$S = 1.039$. The structure was solved with *SHELXS-97*[17] and refined with *SHELXL-97*[17] (CCDB 226253).

Crystal data for **14**. $C_{13}H_{14}N_2O$, $M = 214.26$, tetragonal, space group $P4_1$ (No. 76), $a = b = 12.305(2)$, $c = 7.506(6)$, $U = 1136.5(9)$ Å^3, $Z = 4$, λ(Cu Kα) = 0.643 mm^{-1}, 1558 reflections measured at 180(2) K using an Oxford Cryosystems Cryostream cooling apparatus, 1422 unique ($R_{int} = 0.046$); $R_1 = 0.046$, $wR_2 = 0.116$ [$I > 2\_(I)$]; goodness-of-fit on F^2, $S = 1.059$. The structure was solved with *SHELXS*[17] and refined with *SHELXL*[17] (CCDB 226236).

Acknowledgements

We are grateful to the Engineering and Physical Sciences Research Council of Great Britain for the award of a Studentship (to N.A.) and for financial assistance towards the purchase of the Nonius Kappa CCD diffractometer. L.v.V. is a Benefactor's Scholar of St. John's College, Cambridge and is grateful for support from the Cambridge European Trust in collaboration with the Isaac Newton Trust. L.O. was a summer (2003) project student from the University of Perugia.

REFERENCES

1. Kirby AJ. *Adv. Phys. Org. Chem.* 1980; **17**: 183–278.
2. Kirby AJ. *Acc. Chem. Res*. 1997; **30**: 290–296; Hartwell E, Hodgson DRW, Kirby AJ. *J. Am. Chem. Soc.* 2000; **122**: 9326–9327.
3. Kirby AJ, Percy JM. *J. Chem. Soc., Perkin Trans. 2* 1989; 907–912.
4. Kirby AJ, O'Carroll F. *J. Chem. Soc., Perkin Trans. 2* 1994; 649–655.
5. Gulick AM, Hubbard BK, Gerlt JA, Rayment I. *Biochemistry* 2000; **39**: 4590–4602; St. Maurice M, Bearne SL. *Biochemistry* 2000; **39**: 26.
6. Alder RW, Bowman PS, Steele WRS, Winterman DR. *J. Chem. Soc., Chem. Commun.* 1968; 723–724.
7. Hollfelder F. PhD Thesis, University of Cambridge, 1997.
8. Hodgson DRW, Kirby AJ, Feeder N. *J. Chem. Soc., Perkin Trans. 1* 1999; 949–954.
9. Cho BR, Cho NS, Lee SK. *J. Org. Chem*. 1997; **62**: 2230–2233.
10. Cho BR, Chung HS, Cho NS. *J. Org. Chem.* 1998; **63**: 4685–4690.
11. More O'Ferrall, RA, O'Brien DM, Murphy DG. *Can. J. Chem.* 2000; **78**: 1594–1612.
12. Stewart R. *The Proton: Applications to Organic Chemistry*. Academic Press: New York, 1985.
13. Kirby AJ, Percy JM. *Tetrahedron* 1988; **44**: 6903–6910.
14. Dunitz JD. *X-Ray Analysis and the Structure of Organic Molecules*. Cornell University Press: Ithaca, NY, 1979; 373–375.
15. Grech E, Malarski Z, SawkaDobrowolska W, Sobczyk L. *J. Phys. Org. Chem*. 1999; **12**: 313–318.
16. Kiefl C. *Eur. J. Org. Chem*. 2000; 3279–3286.
17. Sheldrick GM. *SHELXS*-97/*SHELXL*-97. University of Göttingen: Göttingen, 1997.